Engineering Analysis with Boundary Elements 119 (2020) 133–139

Contents lists available at ScienceDirect

Engineering Analysis with Boundary Elements

journal homepage: www.elsevier.com/locate/enganabound

The Erdogan fundamental solution-based hybrid boundary node method for fracture problems

Hai-bin Wang[a], Fei Yan[a,b,c,*], Li-wei Zhang[a], Wei Zhang[a,d], Quan Jiang[a], Zhigang Yan[e], Zhengli Wei[e]

[a] State Key Laboratory of Geomechanics and Geotechnical Engineering, Institute of Rock and Soil Mechanics, Chinese Academy of Sciences, Wuhan 430071, China
[b] CAS center for excellence in Complex System Mechanics, China
[c] Key Laboratory of Ministry of Education on Safe Mining of Deep Metal Mines, Northeastern University, Shenyang 110819, China
[d] University of Chinese Academy of Sciences, Beijing 100049, China
[e] China Railway 12 Bureau Group Co., Ltd, Taiyuan 030024, China

ARTICLE INFO

Keywords:
Linear fracture problems
Erdogan fundamental solutions
Hybrid boundary node method
Origin singular intensity factor
Stress intensity factor

ABSTRACT

Based on the Erdogan fundamental solutions for infinite cracked plates, a new hybrid boundary node method for linear fracture problems is proposed in this paper. The origin singular intensity factor for the Erdogan fundamental solutions is developed to overcome the singular when the field points are coincided with the source points, and no virtual source points are needed, a new scheme for calculating the origin singular intensity factor for the Erdogan fundamental solutions is developed. Based on the Erdogan fundamental solutions, the zero traction boundary condition on crack surfaces is naturally and strictly satisfied in this method, and no nodes are arranged on the crack surface in the entire calculation process. Based on the Erdogan fundamental solution of stress intensity factor for the mixed mode crack, the stress intensity factor of the present method can be easily interpolated by the Erdogan fundamental solutions. As a result, no complex scheme for calculating stress intensity factor is needed. Based on those theories and methods, the proposed method is further applied to analyze some linear crack problems, and the computational accuracy, convergence rate and the versatility of the present method are demonstrated in details.

1. Introduction

As a boundary type meshless method, boundary node method was firstly proposed by Mukherjee [1], in which the moving least square was combined with the boundary integration equations. In this method, only boundary nodes are needed for interpolating boundary variables, but background elements are still needed for local boundary equation integral. In order to overcome this defect, hybrid boundary node method was developed by Zhang et al. [2], in which hybrid displacement variational theory, three fields variables interpolation and moving least square were combined with each other, although no meshing is needed for both variables interpolating and local boundary equation integral, but a boundary layer effect is inevitable. To solve this problem, Zhang and co-workers [3–6] and Wang et al. [7] further proposed the regular hybrid boundary node method, in which the source points are arranged outside the domain, and some virtual source points are needed. Later, employing the rigid body movement method, Miao et al. [8–10] developed a singular boundary node method, in which an adaptive integral scheme to deal with singular integrations and boundary layer effect was developed.

The above methods can only solve the homogenous problems, for inhomogeneous problems, the domain integral and background elements are inevitable. In order to keep the boundary meshless properties of the hybrid boundary node method, Yan et al. [11–13] developed the dual hybrid boundary node method, in which dual reciprocity method [14] was employed into hybrid boundary node method, and furthermore, they employed this method to solve the dynamic problems [15], nonlinear problems [16], convection-diffusion problems [17] and Kirchhoff plates [18]. To improve the calculating effect, the radial point interpolation method was adopted into the dual hybrid boundary node method by Yan et al. [19–23].

Later, Yan et al. [24] proposed a new shape function constructing method, i.e., the Shepard and Taylor interpolation method (STIM) based on the Shepard interpolation method and Taylor expansion, by which no inversion operating is needed in the entire constructing process. Combined multiple reciprocity method [25], Tan et al. [26-27] proposed a

* Corresponding author at: State Key Laboratory of Geomechanics and Geotechnical Engineering, Institute of Rock and Soil Mechanics, Chinese Academy of Sciences, Wuhan 430071, China.

https://doi.org/10.1016/j.enganabound.2020.07.015
Received 4 June 2020; Received in revised form 14 July 2020; Accepted 19 July 2020
Available online 24 July 2020

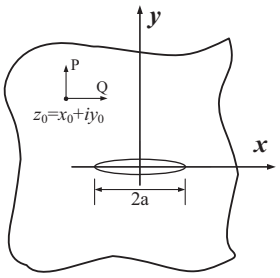

Fig. 1. Infinite plane model with a central crack.

multiple hybrid boundary node method to solve some practical problems. Furthermore, Wang et al. [28-29] developed fast multipole hybrid boundary node method combined fast multipole method [30] and hybrid boundary node method, and employed this method into some complex practical problems [31,32]. Based on those theories, Yan et al. [33] employed hybrid boundary node method and continuous to discontinuous formulation, and proposed a continuous-discontinuous hybrid boundary node method to solve the linear crack problems, in which the field nodes were arranged on the common boundary and the crack surfaces, in this method, the Kelvin fundamental solution was employed, by which the zero traction boundary condition cannot be automatically met, and the stress boundary condition deal is inevitable, because of the singularity of crack tip stress, some special elements are needed to deal with high stress gradient and stress intensity factor calculating.

In order to overcome the aforementioned defects and efficiently solve linear fracture problems, based on the above formulation, the Erdogan fundamental solutions for infinite cracked plates are introduced into the hybrid boundary node method in the present work, and a new hybrid boundary node method for linear fracture problems is proposed. Besides, the concept of the origin singular intensity factor (OSIF) [34,35] is employed into the present method, in which the OSIF for the Erdogan fundamental solutions are developed to overcome the singular when the field points are coincided with the source points, and no virtual source points are needed, a new scheme for calculating the values of OSIF for the Erdogan fundamental solutions is developed. Based on the Erdogan fundamental solutions, the zero traction boundary conditions on crack surfaces are naturally and strictly satisfied, and no nodes are arranged on the crack surface during the calculation, and no special deal is needed for stress boundary condition on crack surfaces. Based on the Erdogan fundamental solution of stress intensity factor (SIF) for the mixed mode crack, the stress intensity factor of the present method can be easily and directly interpolated by the Erdogan fundamental solutions, then no complex scheme for calculating stress intensity factor is needed. Based on those theories and methods, the proposed method will be further applied to analyze some linear crack problems, and the computational accuracy, convergence rate and the versatility of the present method will be demonstrated in details.

2. The Erdogan fundamental solution

Consider an infinite plate with a crack, and a couple of concentrations Q, P is imposed on the point $z_0 = x_0 + iy_0$, which can be seen in Fig. 1. Based on the theory by Erdogan [36], a complex function solution for the above problem can be obtained, then the stress, displacement and stress intensity factor on an arbitrary point $z = x + iy$ on a plane can be given as

$$\sigma_x + \sigma_y = 2\left[\phi(z) + \overline{\phi(z)}\right] \tag{1}$$

$$\sigma_y + i\tau_{xy} = \overline{\phi(z)} + \overline{\Omega(z)} + (\bar{z} - z)\phi'(z) \tag{2}$$

$$2\mu(u + iv) = \kappa \int_0^z \phi(z)dz - \int_0^{\bar{z}} \Omega(\bar{z})d\bar{z} + (\bar{z} - z)\overline{\phi(z)} \tag{3}$$

$$K = K_I - iK_{II} = \frac{1}{2(1+\kappa)\sqrt{\pi a}} \times \left\{ (Q + iP)\left[\left(\frac{a + z_0}{\sqrt{z_0^2 - a^2}} - 1\right) - \kappa\left(\frac{a + \bar{z}_0}{\sqrt{\bar{z}_0^2 - a^2}} - 1\right)\right] + \frac{a(Q - iP)(\bar{z}_0 - z_0)}{(\overline{z_0} - a)\sqrt{\bar{z}_0^2 - a^2}} \right\} \tag{4}$$

in which superscript of horizontal line denotes conjugate function, and superscript of comma represents differential, besides, some other variables can be given as

$$\phi(z) = -\frac{S}{z - z_0} + \phi_0(z) \tag{5}$$

$$\Omega(z) = \frac{\kappa S}{z - \bar{z}_0} + \frac{\bar{S}(\bar{z}_0 - z_0)}{(z - \bar{z}_0)^2} + \phi_0(z) \tag{6}$$

$$\kappa = \begin{cases} 3 - 4\nu \ \textit{plane strain problem} \\ \dfrac{3 - \nu}{1 + \nu} \ \textit{plane stress problem} \end{cases} \tag{7}$$

in which S and $\varphi_0(z)$ in Eqs. (5) and (6) can be written as

$$S = \frac{Q + iP}{2\pi(1 + \kappa)} \tag{8}$$

$$\phi_0(z) = \frac{1}{2\pi\sqrt{z^2 - a^2}} \left\{ \frac{S}{z - z_0}\left[I(z) - I(z_0)\right] - \frac{\kappa S}{z - \bar{z}_0}\left[I(z) - I(\bar{z}_0)\right] - \bar{S}(\bar{z}_0 - z_0)\left[\frac{I(z) - I(\bar{z}_0)}{(z - \bar{z}_0)^2} - \frac{J(\bar{z}_0)}{z - \bar{z}_0}\right] \right\} \tag{9}$$

in which

$$I(z) = \pi\left[\pm\sqrt{z^2 - a^2} - z\right] \tag{10}$$

$$J(z) = \pi\left[\frac{z}{\pm\sqrt{z^2 - a^2}} - 1\right] \tag{11}$$

In those equations, a is the half width of the crack, μ is the shearing modulus, and ν is the Poisson ratio. According to the theory of Erdogan [37] and reference [38], when point z is located on the crack surface, i.e. $-a \le z \le a$, the calculating measure of $I(z)$ and $J(z)$ in Eqs. (9)-(11) are different on the upper and bottom of surfaces. To be specific, when point z is located on the upper side of crack surfaces, a positive sign is used in Eqs. (9)-(11); when point z is located on the bottom side of crack surfaces, a negative sign is used in Eqs. (9)-(11).

Besides, it is worth noting that $\sqrt{z_0^2 - a^2}$ and $\sqrt{\bar{z}_0^2 - a^2}$ result double values in plural space, for example, two solutions can be obtained when calculating $\sqrt{z_0^2 - a^2}$, and square root of this equation can be written as

$$w_k = \sqrt{z^2 - a^2} = \sqrt{r_0}\left[cos\left(\frac{\theta_0}{2} + k\pi\right) + isin\left(\frac{\theta_0}{2} + k\pi\right)\right] \quad k = 1, 2 \tag{12}$$

in which r_0 and θ_0 are modulus and spoke angle of $z^2 - a^2$, respectively. It can be seen that $w_1 = -w_0$ according to Eq. (12). Based on numerical examples, one can see that the value of $\sqrt{z_0^2 - a^2}$ is influenced by the location of point z. For example, $w_0 = \sqrt{z^2 - a^2}$ is used when point z is located in the first quadrant, the fourth quadrant, the positive half of x axis and the positive half of y axis; $w_1 = \sqrt{z^2 - a^2}$ is used when point z is located in the second quadrant, the third quadrant, the negative half of x axis and the negative half of y axis. Based on those results, one can easily use this method.

3. Singular hybrid boundary node method

Three field variable interpolation scheme is used in hybrid boundary node method, then boundary variables and internal variables interpolation are constructed in this section.

3.1. Boundary variable interpolation by radial point interpolation method

The traditional hybrid boundary node method used the moving least square to construct the shape function, and the boundary conditions cannot be easily and directly applied by this method. As a result, the radial point interpolation method (RPIM) is used to interpolate the boundary variable, by which the boundary conditions can be easily and directly applied to the linear equations. Besides, the boundary variables are interpolated on different independent continuous segments, so the boundary is divided into several independent continuous segments.

Take a continuous segment of boundary as an example, then displacement u on this interpolating segment can be written as

$$u(r,s)=\sum_{i=1}^{N_S}R_i(r)a_i+\sum_{j=1}^{m}P_j(s)b_j \tag{13}$$

in which r is the polar coordinate, and s is the parameter coordinate for interpolating point; N_S denotes the node number on interpolating segment, and m is the number of monomials basis; $R_i(r)$ is the radial basis function, which can be seen in references [11], and $P_j(s)=s^{j-1}$, $j=1, 2, \ldots, m$; a_i, b_j are interpolating coefficients.

Applying Eq. (13) into each interpolating node on the interpolating segment, one can get

$$u(r_k,s_k)=\sum_{i=1}^{N_S}R_i(r_k)a_i+\sum_{j=1}^{m}P_j(s_k)b_j \tag{14}$$

As we know, only Eq. (14) can not get the interpolating coefficients, so a constraint of the monomial basis and constant coefficient a_i is built, combining Eq. (14) and this constraint, one can get the system equation of RPIM

$$\begin{Bmatrix}\mathbf{u}_0\\0\end{Bmatrix}=\begin{bmatrix}\mathbf{R}_0 & \mathbf{P}_0\\ \mathbf{P}_0^{\mathrm{T}} & 0\end{bmatrix}\begin{Bmatrix}\mathbf{a}\\\mathbf{b}\end{Bmatrix}=\mathbf{G}\mathbf{a}_0 \tag{15}$$

in which $\mathbf{a}_0^{\mathrm{T}}=[a_1,a_2,\ldots,a_{N_S},b_1,b_2,\ldots,b_m]$, and $\mathbf{R}_0$ and $\mathbf{P}_0$ are the matrixes of values for radial basis functions and the monomials basis on each interpolating nodes respectively, based on Eq. (15), one can get the interpolating coefficients $\mathbf{a}_0=\mathbf{G}^{-1}\mathbf{u}_0$. Substituting this interpolating coefficient into Eq. (13), one can get the shape function of RPIM, which can be written as

$$\begin{aligned}\mathbf{\Phi}^{\mathrm{T}}(r,s)&=\left[\phi_1(r,s),\phi_2(r,s),\ldots,\phi_{N_S}(r,s),\ldots,\phi_{N_S+m}(r,s)\right]\\&=\left[\mathbf{R}^{\mathrm{T}}(r)\mathbf{P}^{\mathrm{T}}(s)\right]\mathbf{G}^{-1}\end{aligned} \tag{16}$$

According to Eq. (16), the boundary variables can be interpolated via the above shape function, then one can obtain

$$\tilde{\mathbf{u}}(r,s)=\mathbf{\Phi}^{\mathrm{T}}(r,s)\mathbf{u} \tag{17}$$

in which $\mathbf{u}^{\mathrm{T}}=[u_1,u_2,\ldots,u_{N_S}]$ is displacement vector for boundary nodes. The same as Eq. (17), boundary variables of traction can also be interpolated by the same shape function,

$$\tilde{\mathbf{t}}(r,s)=\mathbf{\Phi}^{\mathrm{T}}(r,s)\mathbf{t} \tag{18}$$

in which $\mathbf{t}^{\mathrm{T}}=[t_1,t_2,\ldots,t_{N_S}]$ is traction vector for boundary nodes.

3.2. Internal variable interpolation based on OSIF

Internal variable interpolation in traditional hybrid boundary node method is based on fundamental solution interpolation, but singular or near singular cases can occur when the source points and the field points coincide with each other. In order to overcome this problem, Yan et al. [38] proposed a dual singular hybrid boundary node method, in which the origin singular intensity factor is employed, and the calculating scheme of OSIF for potential problems is given in this work, and in this section, the calculating scheme of OSIF for the Erdogan fundamental solutions is developed.

According to the theory of the origin singular intensity factor, the internal variables can be interpolated by

$$u(z_I)=\sum_{J=1,J\neq I}^{N}U(z_I,z_J)x_J+OIFU(z_I,z_I)x_I \tag{19}$$

$$v(z_I)=\sum_{J=1,J\neq I}^{N}V(z_I,z_J)x_J+OIFV(z_I,z_I)x_I \tag{20}$$

$$t_i(z_I)=\sum_{J=1,J\neq I}^{N}G_i(z_I,z_J)x_J+OIFT(z_I,z_I)x_I \tag{21}$$

in which N is the total boundary node number, $U(z_I,z_J)$,$V(z_I,z_J)$ are the Erdogan fundamental solution of displacements for x and y direction, which can be solved by Eq. (3), $G_i(z_I,z_J)$ is the Erdogan fundamental solution of traction, which is related to σ_x, σ_y, τ_{xy}, and the relation is $G_i(z_I,z_J)=\sigma_{ij}(z_I,z_J)n_j$, and n_j is the outward normal vector component of boundary, and $OIFU(z_I,z_I)$, $OIFV(z_I,z_I)$, $OIFT(z_I,z_I)$ are origin singular intensity factor of displacement and traction, and x_I is the interpolation coefficient.

As we know, after substituting the source point and the field point into Eqs. (1) to (12), the value of the Erdogan fundamental solutions can be easily got, but from those equations, one can not easily get the analytical form of the Erdogan fundamental solutions. As a result, the main problem is solving the origin singular intensity factor in Eqs. (19) to (21). According to reference [37], one can see that the OSIF exists, and it is not infinite. Then the method of fundamental solution is used to solve the origin singular intensity factor. In the present work, the mixed mode displacement, stress field of crack tip are used as the simple field functions, which can be given as

$$u_x=\frac{K_I}{2\mu}\sqrt{\frac{r}{2\pi}}\cos\frac{\theta}{2}\left(\kappa-1+2\sin^2\frac{\theta}{2}\right)+\frac{K_{II}}{2\mu}\sqrt{\frac{r}{2\pi}}\sin\frac{\theta}{2}\left(\kappa+1+2\cos^2\frac{\theta}{2}\right) \tag{22}$$

$$u_y=\frac{K_I}{2\mu}\sqrt{\frac{r}{2\pi}}\sin\frac{\theta}{2}\left(\kappa+1-2\cos^2\frac{\theta}{2}\right)-\frac{K_{II}}{2\mu}\sqrt{\frac{r}{2\pi}}\cos\frac{\theta}{2}\left(\kappa-1-2\sin^2\frac{\theta}{2}\right) \tag{23}$$

$$\sigma_x=\frac{K_I}{\sqrt{2\pi r}}\cos\frac{\theta}{2}\left(1-\sin\frac{\theta}{2}\sin\frac{3\theta}{2}\right)+\frac{K_{II}}{\sqrt{2\pi r}}\sin\frac{\theta}{2}\left(2+\cos\frac{\theta}{2}\cos\frac{3\theta}{2}\right) \tag{24}$$

$$\sigma_y=\frac{K_I}{\sqrt{2\pi r}}\cos\frac{\theta}{2}\left(1+\sin\frac{\theta}{2}\sin\frac{3\theta}{2}\right)+\frac{K_{II}}{\sqrt{2\pi r}}\sin\frac{\theta}{2}\cos\frac{\theta}{2}\cos\frac{3\theta}{2} \tag{25}$$

$$\tau_{xy}=\frac{K_I}{\sqrt{2\pi r}}\sin\frac{\theta}{2}\cos\frac{\theta}{2}\cos\frac{3\theta}{2}+\frac{K_{II}}{\sqrt{2\pi r}}\cos\frac{\theta}{2}\left(1-\sin\frac{\theta}{2}\sin\frac{3\theta}{2}\right) \tag{26}$$

in which $K_I=1$, $K_{II}=1$ are used in the present method.

In order to solve the OSIF, some calculating points are arranged in the calculating domain, and it is assured that the distances from calculating points to the source points are larger than half of the adjacent nodal distance of boundary nodes, and the calculating node number is N_c, which is much larger than the total number of boundary nodes N, in other words, $N_c \geq N$. In this case, an interpolation scheme based on the method of fundamental solution can be built, which can be given as

$$u_c(z_i)=\sum_{J=1}^{N}U(z_i,z_J)\alpha_J \tag{27}$$

$$t_c(z_i)=\sum_{J=1}^{N}T(z_i,z_J)\beta_J \tag{28}$$

Substituting Eqs. (22) and (23) into Eq. (27), one can get

$$\begin{bmatrix} U(z_1,z_1) & U(z_1,z_2 & \dots & U(z_1,z_N) \\ U(z_2,z_1) & U(z_2,z_2) & \dots & U(z_2,z_N) \\ \vdots & \vdots & \ddots & \vdots \\ U(z_{N_c},z_1) & U(z_{N_c},z_2) & \dots & U(z_{N_c},z_N) \end{bmatrix} \begin{Bmatrix} \alpha_1 \\ \alpha_2 \\ \vdots \\ \alpha_N \end{Bmatrix} = \begin{Bmatrix} u_c(z_1) \\ u_c(z_2) \\ \vdots \\ u_c(z_{N_c}) \end{Bmatrix} \tag{29}$$

From Eq. (27), one can easily obtain the interpolation coefficient, then one can get the OSIF of displacement, which is

$$OIFU(z_I,z_I) = \frac{u_c(z_I) - \sum_{J=1,J\neq I}^{N} U(z_I,z_J)\alpha_J}{\alpha_I} \tag{30}$$

Using the same method, one can easily get the interpolating coefficient, then the OSIF of stress can also be obtained as

$$OIFG_x(z_I,z_I) = \frac{\sigma_x(z_I) - \sum_{J=1,J\neq I}^{N} G_x(z_I,z_J)\beta_J}{\beta_I} \tag{31}$$

$$OIFG_y(z_I,z_I) = \frac{\sigma_y(z_I) - \sum_{J=1,J\neq I}^{N} G_y(z_I,z_J)\beta_J}{\beta_I} \tag{32}$$

$$OIFG_{xy}(z_I,z_I) = \frac{\tau_{xy}(z_I) - \sum_{J=1,J\neq I}^{N} G_{xy}(z_I,z_J)\beta_J}{\beta_I} \tag{33}$$

Based on $OIFT(z_I,z_I) = OIFG_{ij}(z_I,z_J)n_j$, one can get the origin intensity factor of traction.

3.3. Singular hybrid boundary node method

According to the hybrid displacement variational theory, the local boundary integral equation can be given as

$$\int_{\Gamma_S} (t-\tilde{t})h_J(Q)d\Gamma = 0 \tag{34}$$

$$\int_{\Gamma_S} (u-\tilde{u})h_J(Q)d\Gamma = 0 \tag{35}$$

in which $h_J(Q)$is the test function, and the complete function can be referred as references [11-13], u, t are displacement and traction on internal points, which are interpolated by Eqs. (19)-(21), $\tilde{u}$, $\tilde{t}$ are displacement and traction on boundary nodes, which are interpolated by RPIM, and they are based on Eqs. (17) and (18).

Substituting Eqs. (17) – (21) into Eqs. (34) and (35), one can get the linear system equation of the present method, which are

$$\mathbf{Tx} = \mathbf{Ht} \tag{36}$$

$$\mathbf{Ux} = \mathbf{Hu} \tag{37}$$

in which matrices **T, U, H** can be referred in references [11-13].

Based on Eqs. (19)-(21), one can get the field function of stress, displacement on any points, which can be written as

$$u_i(z_I) = \sum_{J=1,J\neq I}^{N} U_i(z_I,z_J)x_J + OIFU(z_I,z_I)x_I \tag{38}$$

$$t_i(z_I) = \sum_{J=1,J\neq I}^{N} G_i(z_I,z_J)x_J + OIFT(z_I,z_I)x_I \tag{39}$$

Different from the traditional hybrid boundary node method, only boundary nodes are needed in the present method, and the zero traction on crack surfaces can be automatically satisfied, and no crack surface elements are needed.

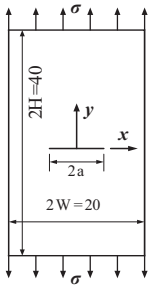

Fig. 2. Pure mode I central cracked plane.

4. Implementation for SBNM

For linear fracture problems, the main problem is calculating stress intensity factor. Different from some other methods, it can be seen in Eq. (4) that the fundamental solution of stress intensity factor can be obtained from the Erdogan fundamental solutions. Based on Eqs. (19)-(21), one can get

$$K_I(z_I) = \sum_{J=1}^{N} K_I^E(z_I,z_J)x_J \tag{40}$$

$$K_{II}(z_I) = \sum_{J=1}^{N} K_{II}^E(z_I,z_J)x_J \tag{41}$$

in which $K_I^E(z_I,z_J)$, $K_{II}^E(z_I,z_J)$ are the Erdogan fundamental solutions of stress intensity factor, x_J is the interpolating coefficient. Because the calculating points are located in the internal of calculating domain, then no singular is occurred all over the interpolating process, then no OSIF for stress intensity factor is needed.

In the Erdogan fundamental solutions, the analytical functions can not be easily obtained from Eqs. (1)-(12). In other words, the analytical function is not needed for calculating. Only the values on different points are needed for the whole calculating, then, one can only substitute the coordinate of the source points and the field points into Eqs. (1)-(12), and using the theory of complex function, each different values of the Erdogan fundamental solutions can be separated by Eqs. (1)-(20).

For simplification, a dimensionless stress intensity factor is defined, which is

$$\hat{K}_{I,II} = \frac{K_{I,II}}{\sigma\sqrt{\pi a_0}} \tag{42}$$

in which σ is the far field stress, and a_0 is the total length of crack.

5. Numerical examples

In this section, several numerical examples are given to illustrate the accuracy and effectiveness of the present method.

5.1. Mode I central cracked plane

A pure mode I central cracked plane is considered in this example, which can be seen in Fig. 2, and $2a$, $2W$, $2H$ are crack length, width and height of the crack plane, and $\sigma = 1$ is considered in this section. Besides, different crack lengths are considered for comparison purpose.

Fig. 3 plots the relative errors for different crack lengths and different boundary node numbers, it can be seen in this figure that convergence of the present method is quick, and the accuracy of the present method is high, and when the boundary node number is more than 90, the relative error decreases much slower.

Fig. 4 shows the dimensionless stress intensity factor for different crack lengths, and it can be seen that the present method is very close to the analytical solution and results by Spline fictitious boundary element method (SFBEM) [37], which illustrates that the present method

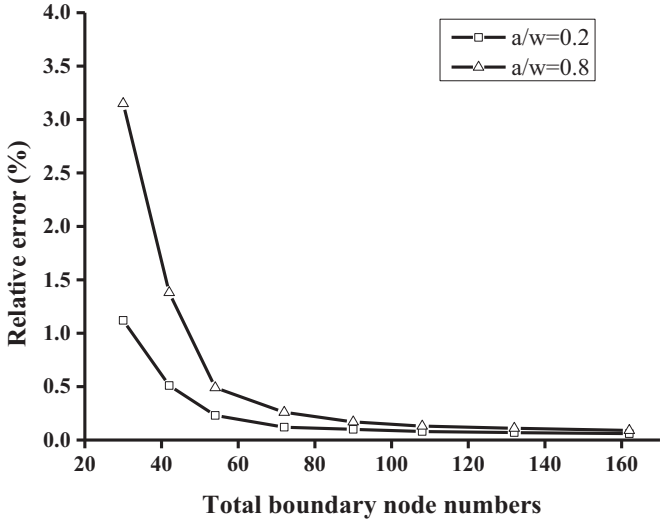

Fig. 3. Relative errors for different boundary node numbers and different crack lengths.

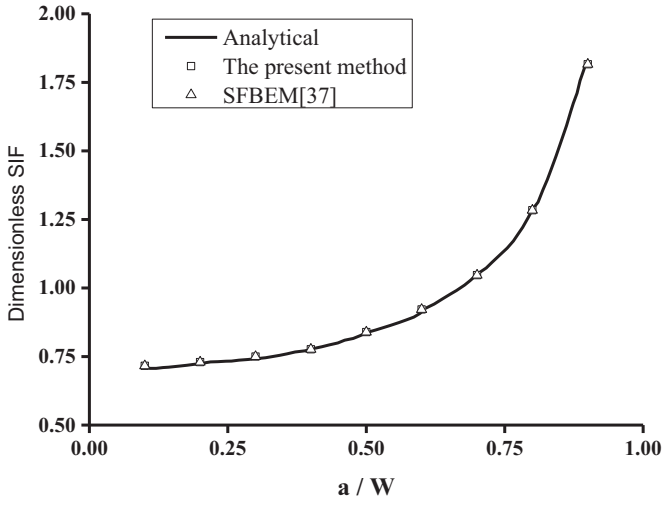

Fig. 4. Dimensionless SIF for different crack lengths.

is accurate and effective, compared to the traditional hybrid boundary node method, only boundary nodes are arranged for calculating, and no crack surface nodes are needed, and the zero traction boundary condition for crack surfaces is automatically satisfied.

5.2. Single-sided inclined crack rectangular plate

A rectangular plate with a single-sided inclined crack is considered in this example, which can be seen in Fig. 5. a is crack length, W is width of the plate, the plate height is $2.5H$, $\sigma = 1$, and the inclined angle to vertical direction is $0^\circ < \beta \leq 90^\circ$, representing a mixed mode fracture problem.

In the present method, a total of 144 boundary nodes are used in this example, crack inclined angles $\beta = 45^\circ$, $\beta = 67.5^\circ$ and $\beta = 90^\circ$ are considered, which are the same as the above example. Results by SFBEM [37] are employed for comparison.

Figs. 6 and 7 plot the results of dimensionless stress intensity factor by the present method, SFBEM and analytical solution, in which a great agreement can be achieved, which illustrates that the present method is accurate and effective. Compared to the traditional method, no meshing is needed on crack surfaces in the present method.

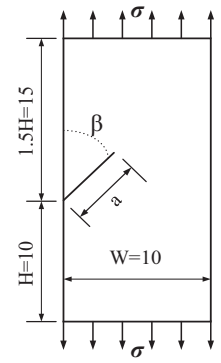

Fig. 5. Single-sided inclined crack rectangular plate.

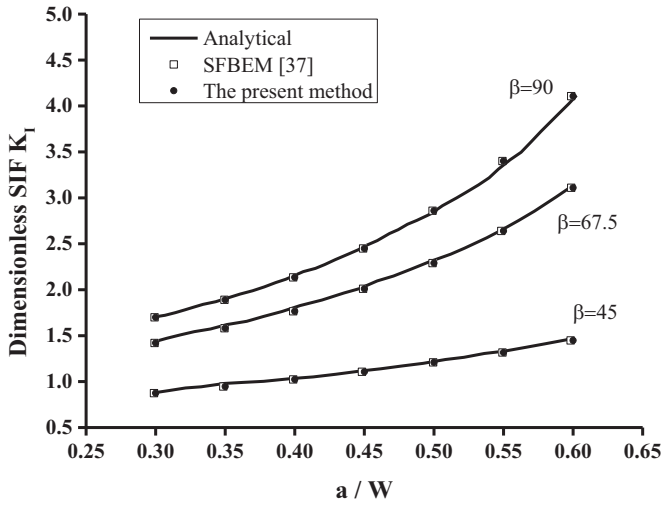

Fig. 6. Values of $\hat{K}_I$ for different crack inclined angles β.

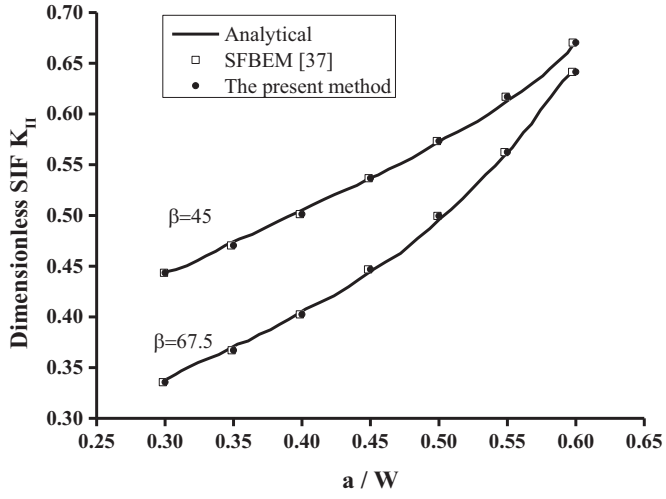

Fig. 7. Values of $\hat{K}_{II}$ for different crack inclined angles β.

5.3. A central inclined cracked plate

Fig. 8 shows an angle-cracked plate with the length $2b = 20m$ and the width $2h = 30m$. The crack length is $2a = 3m$, and the angle between crack direction and vertical direction is α. The far field tensile is $\sigma = 1Pa$.

Fig. 9 shows the stress intensity factor K_I and K_{II} for different inclined angles α, it can be seen that results by the present method are very

Table 1
Dimensionless stress intensity factors for a central inclined plate.

Angle α	$\tilde{K}_I = K_I/K_I^A$			$\tilde{K}_{II} = K_{II}/K_{II}^A$		
	Present method	HBNM[23]	XFEM[39]	Present method	HBNM[23]	XFEM[39]
15	0.983	1.021	1.034	0.988	1.013	0.979
30	1.010	1.009	1.011	1.007	1.005	1.006
45	1.005	1.007	0.991	1.012	1.028	0.922
60	1.009	1.011	1.017	1.008	1.007	1.013
75	0.985	1.014	1.019	0.983	1.020	1.033

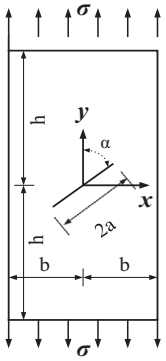

Fig. 8. Central inclined cracked plate under tensile.

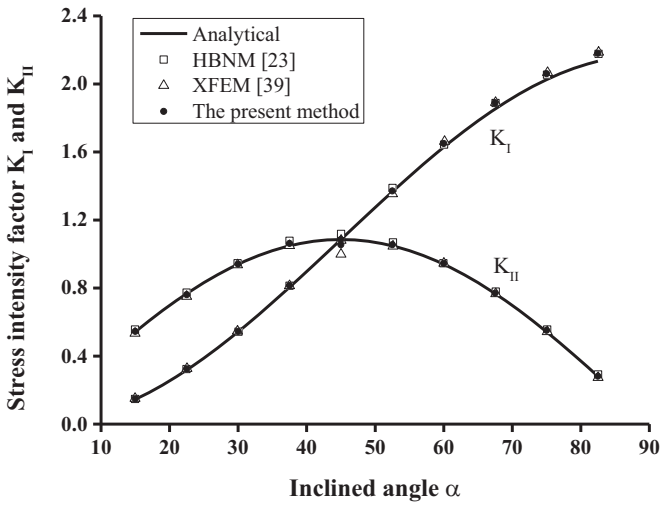

Fig. 9. Stress intensity factor for a central inclined plate on different inclined angles.

close to analytical solutions, results by extended finite element method (XFEM) [39] and the traditional hybrid boundary node method [23], which reveals that the present method can achieve a great accurate and effective, because only 88 boundary nodes are needed for the whole calculating, but 120 boundary nodes are needed on boundary and crack surfaces by the traditional hybrid boundary node method. Table 1 shows the dimensionless stress intensity factors, in which results by the traditional hybrid boundary node method and XFEM are also given for comparison, and one can see that the present method can get much more accurate results compared to the other two methods.

5.4. Panel with doubly cracked hole

In this section, a panel which contains a doubly-cracked hole is considered, which is shown in Fig. 10, and a uniaxial tensile σ is imposed on the upper and bottom sides of the plate. The geometry of the calculating domain is given as: $2h/W = a/r = 1$, and $r + a = W/4$. Results by Chang and Mear [40], Pan [41] are given for comparison, and the continuous-discontinuous hybrid boundary node method results by Yan et al. [23] are also presented in this section.

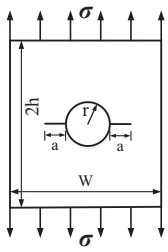

Fig. 10. Panel with a doubly cracked hole.

Table 2
Stress intensity factors for the doubly cracked hole.

Method	$K_I/\sigma\sqrt{\pi(r+a)}$
The present method	1.5633
DHBNM with Quadratic basis [23]	1.6029
DHBNM with enriched basis [23]	1.5632
BEM by Chang and Mear[40]	1.5627
BEM by Pan [41]	1.5636

The stress intensity factor for the doubly-cracked hole is shown in Table 2, in which results by some other methods are given for comparison. It can be seen that the results obtained by the present method are well agreed between those four different methods. For simplification, a half model of Fig. 10 is considered in the present work, and a total of 101 boundary nodes are used for calculating, and in the present method no crack surface nodes are needed. For the traditional hybrid boundary node method, a total of 150 boundary nodes were used [23], and crack surface elements are inevitable for zero traction boundary conditions.

6. Conclusions

In the present work, the Erdogan fundamental solutions for infinite cracked plates are introduced to the hybrid boundary node method, and a new hybrid boundary node method for linear fracture problems is proposed. Firstly, the concept of the origin singular intensity factor is employed into the present method, in which the OSIF for the Erdogan fundamental solutions is developed to overcome the singular when the field points coincide with the source points, and no virtual source points are needed, and a new scheme for calculating the values of OSIF for the Erdogan fundamental solutions is proposed. Because the zero traction boundary condition on crack surfaces is naturally and strictly satisfied, no nodes are arranged on the crack surfaces in the entire calculating process, and no special deal is needed for stress boundary condition on crack surfaces. Based on the Erdogan fundamental solution of stress intensity factor for the mixed mode crack, the stress intensity factor of the present method can be easily and directly interpolated by the Erdogan fundamental solutions, and no complex scheme for calculating stress

intensity factor is needed. Based on the aforementioned theories and methods, the proposed method is applied to analyze some linear crack problems, and numerical examples are given to illustrate that the computational accuracy, convergence rate and the versatility of the present method are very high, and it can be further used for practical engineering operations.

Declaration of Competing Interest

The authors have no conflict of interest.

Acknowledgments

This work was supported by the National Natural Science Foundation of China (Grant Nos. 41572296, 51621006), State Key Research Development Program of China (Grant No. 2017YFC0804203), Key Research Program of Frontier Sciences, Chinese Academy of Sciences (Grant No. QYZDB-SSW-DQC029), and Grant from Department of Science and Technology of Shaanxi Province (2020JQ-999).

References

[1] Mukherjee YX, Mukherjee S. The boundary node method for potential problems. Int J Num methods Eng 1997;40:797–815.
[2] Zhang JM, Yao ZH, Li H. A Hybrid boundary node method. Int J Num methods Eng 2002;53:751–63.
[3] Zhang JM, Yao ZH, Masataka T. The meshless regular hybrid boundary node method for 2-D linear elasticity. Eng Anal Bound Elem 2003;127:259–68.
[4] Zhang JM, Yao ZH. The regular hybrid boundary node method for three-dimensional linear elasticity. Eng Anal Bound Elem 2004;28:525–34.
[5] Zhang JM, Masataka T, Toshiro M. Meshless analysis of potential problems in three dimensions whit the hybrid boundary node method. Int J Num Meth Eng 2004;59:1147–68.
[6] Zhang JM, Yao ZH. Meshless regular hybrid boundary node method. Comput Model Eng Sci 2001;2:307–18.
[7] Wang HT, Yao ZH, Cen S. A meshless singular hybrid boundary node method for 2-D elatostatics. J Chin Inst Eng 2004;27:481–90.
[8] Miao Y, Wang YH, Yu F. An improved hybrid boundary node method in two-dimensional solids. Acta Mech Solida Sin 2005;18:307–15.
[9] Miao Y, Wang Q, Zhu HP. Thermal analysis of 3d composites by a new fast multipole hybrid boundary node method. Comput Mech 2014;53:77–90.
[10] Miao Y, Sun TC, Zhu HP, Wang Q. A new model for the analysis of reinforced concrete members with a coupled HdBNM/FEM. Appl Math Model 2014;38:5582–91.
[11] Yan F, Feng XT, Zhou H. A dual reciprocity hybrid radial boundary node method based on radial point interpolation method. Comput Mech 2010;45:541–52.
[12] Yan F, Wang YH, Tham LG, Cheung YK. Dual reciprocity hybrid boundary node method for 2-D elasticity with body force. Eng Anal Bound Elem 2008;32:713–25.
[13] Yan F, Wang YH, Miao Y, Tan F. Dual reciprocity hybrid boundary node method for three-dimensional elasticity with body force. Acta Mech Solida Sin 2008;21:267–77.
[14] Nardini D, Brebbia CA. Transient dynamic analysis by the boundary element method. Boundary element methods in engineering. Southampton: computational mechanics publications. Berlin and New York: Springer; 1983.
[15] Yan F, Wang YH, Miao Y, Cheung YK. Dual reciprocity hybrid boundary node method for free vibration analysis. J Sound Vib 2009; 321: 1036-1057
[16] Yan F, Miao Y, Yang QN. Quasilinear hybrid boundary node method for solving nonlinear problems. CMES-Comput Model Eng Sci 2009;46(1):21–50.
[17] Yan F, Yu M, Lv JH. Dual reciprocity boundary node method for convection-diffusion problems. Eng Anal Bound Elem 2017;80:230–6.
[18] Yan F, Feng XT, Zhou H. Dual reciprocity hybrid radial boundary node method for the analysis of Kirchhoff plates. Appl Math Model 2011;35(12):5691–706.
[19] Yan F, Feng XT, Zhou H. Dual reciprocity hybrid radial boundary node method for Winkler and Pasternak foundation thin plate. Arch Appl Mech 2013;83(2):225–39.
[20] Yan F, Pan PZ, Feng XT, Li SJ, Jiang Q. A fast successive relaxation updating method for continuous-discontinuous cellular automaton method. Appl Math Model 2019;66:156–74.
[21] Wang HB, Yan F, Li XC, et al. Evolution mechanism study of flow-slide catastrophes in large waste dumps at the Nanfen iron mine. B Eng Geol Environ 2020. doi:10.1007/s10064-020-01881-0.
[22] Jiang Quan, Yang Bing, Yan Fei, et al. New method for characterizing the shear damage of natural rock joint based on 3d engraving and 3d scanning. Int J Geomech 2020;20(2):06019022.
[23] Yan F, Pan PZ, Feng XT, Li SJ. The continuous-discontinuous cellular automaton method for elastodynamics crack problems. Eng Fract Mech 2018;204:482–96.
[24] Yan F, Feng XT, Lv JH, Pan PZ. A new hybrid boundary node method based on Taylor expansion and Shepard interpolation method. Int J Numer Meth Eng 2015;102:1488–506.
[25] Neves AC, Brebbia CA. The multiple reciprocity method applied to thermal stress problems. Int J Num Meth Eng 1992;35(3):443–55.
[26] Tan F, Wang SF, Lv JH, Jiao YY. A Galerkin boundary cover method for viscous fluid flows. Eur J Mech B Fluid 2019;78:174–81.
[27] Tan F, Wang YH. Multiple reciprocity hybrid boundary node method for potential problems. Eng Anal Bound Elem 2010;34:369–76.
[28] Wang Q, Yang HY. A rigid-inclusion model for fiber-reinforced composites by fast multipole hybrid boundary node method. Eng Anal Bound Elem 2015;54:76–85.
[29] Wang Q, Miao Y, Zhu HP. A new formulation for thermal analysis of composites by hybrid boundary node method. Int J Heat Mass Transf 2013;64:322–30.
[30] Coifman R. The fast multipole method for the wave equation: a pedestrian prescription. IEEE Trans Antennas Propag Mag 1993:35.
[31] Wang Q, Zhou W, Feng YT. The phase-field model with an auto-calibrated degradation function based on general softening laws for cohesive fracture. Appl Math Model 2020;86:185–206.
[32] Zhou W, Liu B, Wang Q, Chang XL, Chen XD. Formulations of displacement discontinuity method for crack problems based on boundary element method. Eng Anal Bound Elem 2020;115:86–95.
[33] Yan F, Feng XT, Lv JH, Li SJ. The continuous-discontinuous hybrid boundary node method for solving stress intensity factor. Eng Anal Bound Elem 2017;81:35–43.
[34] Chen W, Fu Z, Wei X. Potential problems by singular boundary method satisfying moment condition. Comput Model Eng Sci 2009;54:65–85.
[35] Wei X, Chen W, Sun LL, Chen B. A simple accurate formula evaluating origin intensity factor in singular boundary method for two-dimensional potential problems with Dirichlet boundary. Eng Anal Bound Elem 2015;58:151–65.
[36] Erdogan F. On the stress distribution in a plate with collinear cuts under arbitrary loads. In: Proc. 4th US national congress of applied mechanics; 1962. p. 547–53.
[37] Su C, Zheng C. Calculating of stress intensity factors by boundary element method based on Erdogan fundamental solutions. Chin J Theor Appl Mech 2007;39(1):93–9.
[38] Yan F, Jiang Q, Li SJ, Pan PZ, Xu DP, Zhang JX, Fan B. A dual singular hybrid boundary node method based on origin singular intensity factor. Eng Anal Bound Elem 2020.
[39] Dong YW, Yu TT, Ren QW. Extended finite element method for direct evaluation of strength intensity factors. Chin J Comput Mech 2008;25(1):72–7.
[40] Chang CC, Mear ME. A boundary element method for two dimensional linear elastic fracture analysis. Int J Fract 1995;74:219–51.
[41] Pan E. A general boundary element analysis of 2-D linear elastic fracture mechanics. Int J Fract 1997;88 41-59s.